# Objective activity parameters track patient-specific physical recovery trajectories after surgery and link with individual preoperative immune states

Ramin Fallahzadeh[1,2]*, PhD; Franck Verdonk[1]*, MD, PhD; Ed Ganio[1], PhD; Anthony Culos[12] BS; Natalie Stanley[3], PhD; Ivana Marić[4], PhD; Alan L. Chang[12], PhD; Martin Becker[12], PhD; Thanaphong Phongpreecha[125], PhD; Maria Xenochristou[12], PhD; Davide De Francesco[12], PhD; Camilo Espinosa[12], BS; Xiaoxiao Gao[1], BS; Amy Tsai[1], BS; Pervez Sultan[1], MD, PhD; Martha Tingle[1], RN; Derek F. Amanatullah[6], MD, PhD; James I. Huddleston[6], MD; Stuart B. Goodman[6], MD, PhD; Brice Gaudilliere[1,4‡], MD, PhD; Martin S. Angst[1‡], MD, PhD; Nima Aghaeepour[1,2,4‡], PhD

[1]Department of Anesthesiology, Pain and Perioperative Medicine, Stanford University

[2]Department of Biomedical Data Science, Stanford University

[3]Department of Computer Science, University of North Carolina at Chapel Hill

[4]Department of Pediatrics, Stanford University

[5]Department of Pathology, Stanford University

[6]Department of Orthopedic Surgery, Stanford University

*co-first author

‡co-senior author

Corresponding author: Nima Aghaeepour, 300 Pasteur Drive, Grant S280, Stanford, CA, USA, 94305-5117. Tell: (650) 497- 0410.

**Running head:** Wearables to track individual recovery trajectories

Author contributions: R.F., F.V., E.G., N.S., I.M., A.L.C., M.B., T.P., M.X., D.D.F., C.E., P.S., D.F.A., J.I.H., S.B.G., B.G., M.S.A., and N.A. contributed to conception and design. E.G., X.G., A.T., M.T., B.G., M.S.A, and N.A. acquired the data. R.F., F.V., A.C., B.G.,

M.S.A, and N.A. analyzed the data and interpreted the results. R.F., F.V., B.G., M.S.A., and N.A. wrote the manuscript with input from all authors.

## Mini-Abstract

Objective and high-fidelity parameters were studied in surgical patients using wearable technology to derive patient-specific physical recovery trajectories. A multi-parameter model outperformed benchmark metrics and linked individual trajectories to preoperative immune states.

## Abstract

**Objective:** The longitudinal assessment of physical function with high temporal resolution at a scalable and objective level in patients recovering from surgery is highly desirable to understand the biological and clinical factors that drive the clinical outcome. However, physical recovery from surgery itself remains poorly defined and the utility of wearable technologies to study recovery after surgery has not been established.

**Background:** Prolonged postoperative recovery is often associated with long-lasting impairment of physical, mental, and social functions. While phenotypical and clinical patient characteristics account for some variation of individual recovery trajectories, biological differences likely play a major role. Specifically, patient-specific immune states have been linked to prolonged physical impairment after surgery. However, current methods of quantifying physical recovery lack patient specificity and objectivity.

**Methods:** Here, a combined high-fidelity accelerometry and state-of-the-art deep immune profiling approach was studied in patients undergoing major joint replacement surgery. The aim was to determine whether objective physical parameters derived from accelerometry data can accurately track patient-specific physical recovery profiles (suggestive of a 'clock of postoperative recovery'), compare the performance of derived parameters with benchmark metrics including step count, and link individual recovery profiles with patients' preoperative immune state.

**Results:** The results of our models indicate that patient-specific temporal patterns of physical function can be derived with a precision superior to benchmark metrics. Notably, six distinct domains of physical function and sleep are identified to represent the objective temporal patterns: "activity capacity" and "moderate and overall activity" (declined immediately after surgery); "sleep disruption and sedentary activity" (increased after surgery); "overall sleep", "sleep onset", and "light activity" (no clear changes were observed after surgery). These patterns can be linked to individual patients' preoperative immune state using cross-validated canonical-correlation analysis. Importantly, the pSTAT3 signal activity in M-MDSCs predicted a slower recovery.

**Conclusions:** Accelerometry-based recovery trajectories are scalable and objective outcomes to study patient-specific factors that drive physical recovery.

## Introduction

Currently, more than 300 million surgeries are performed annually worldwide [1]. Recovery after surgery is highly variable, and protracted recovery affects up to 30% of patients, leading to personal suffering, impaired daily function, delayed return to work, and major socioeconomic costs [2]–[4]. While rapid advances in surgical and perioperative care have significantly shortened hospital length of stay, surgical recovery far exceeds the hospitalization period [5], [6]. From a patient's perspective, recovery includes the return to preoperative levels of independence and well-being [7]. As such, studying the entire surgical recovery process, which can last weeks to months, is logistically challenging, resource-intense, and largely contingent on subjective data typically obtained with questionnaires [8]–[11]. Additional concerns regarding subjective data include reporting biases and limited reliability [12]. For example, self-reported physical performance metrics are imprecise as they both, under and overestimate activity when compared to objective metrics [12], [13]. Finally, a large-scale study conducted in six countries comparing subjective and survey-based physical activity metrics to sensor-based metrics of physical activity that measured time spent in sedentary behavior and specific intensity levels of physical activity (light, moderate, and vigorous), indicated a large discordance between self-reported and sensor-based outcomes [13].

One sentinel recovery outcome after surgery is physical function, which is likely to impact other domains of recovery. The scalable, low-cost, objective, remote, and continuous assessment of physical function over extended periods of time is highly desirable to understand mechanisms that improve, or conversely, impede physical function. As such, the application of sensing technologies included in wearable devices for monitoring of physical function is rapidly emerging in different clinical domains including inpatient rehabilitation, sleep, geriatric, and feto-maternal medicine [14] [15][16]. However, the utility of wearable technologies to study recovery after surgery has not been established.

The role of the immune system in determining recovery in patients suffering from trauma including major surgery is prominent [17]–[19]. Mass cytometry [20], a recent breakthrough technology for highly parameterized single-cell immune profiling has rapidly been adopted in different clinical settings including vaccine development [21], feto-maternal health [22], [23], oncology and immunotherapy [24]. More recently, mass cytometry has been used in perioperative medicine, by our group, to study how a patient's preoperative immune state and immune responses to surgery determine clinical recovery trajectories (derived from self-reported measurements) [19], [25]. Evidence from these important and resource-intense but limited-sized studies suggests that patient-specific differences in immune cell signaling responses are strongly associated with the rate at which patients regain physical function after surgery.

Here, a novel patient-centric computational approach is presented that leverages wearable acceleration data and high-parameter functional immune profiling to (1) objectively quantify the temporal pattern of physical recovery in individual patients (suggestive of a 'clock of

postoperative recovery' indicating time to return to their preoperative state), and (2) link such recovery patterns to individual patients' preoperative immune states. Integration of accelerometry and biological data is a novel and personalized framework to identify biological factors that drive physical recovery. The outlined approach, once validated, can be scaled to larger and more diverse surgical cohorts with the final goal to advance physical recovery in a personalized and preemptive fashion.

## Methods

### Clinical study design

Patients undergoing primary hip arthroplasty (PHA) were recruited at the Arthritis and Joint Replacement Clinic of the Department of Orthopedic Surgery at Stanford University School of Medicine (see "CONSORT Chart" and "Study Materials" in Supplementary Content, http://links.lww.com/SLA/D476). The study was approved by the Institutional Review Board of Stanford University. Seventy-five patients were enrolled after providing written informed consent. Fifty-three patients completed the study and 49 patients provided accelerometry data suitable for analysis (Table 1). Refer to "Study Materials" in Supplementary Content for the exclusion criteria.

### Accelerometry for measurement of physical activity and sleep patterns

Physical activity and sleep patterns of each participant were collected via an ActiGraph smartwatch (ActiGraph, LLC, FL, USA) continuously worn on the wrist of the dominant arm starting 5 days before surgery and ending forty days after surgery (Figure 1A). Two patients wore the watch on the non-dominant wrist. The three-dimensional acceleration data were sampled at 30 Hz, which produced about 350 million acceleration measurements per patient. A broad array of algorithms extracted time-series attributes (or features) representing various aspects of daily physical activity (e.g., step counts, energy expenditure, and time spent at various physical activity levels) as well as sleep features. For example, the Cole-Kripke algorithm [26] and the Freedson algorithm [27] were used for deriving sleep and energy expenditure features, respectively. A complete list of features is provided in Supplementary Table 1, http://links.lww.com/SLA/D476. ActiGraph's actigraphy data analysis software platform ActiLife v6.13.3 was used for the purpose of feature extraction. Missing values were imputed using a 2-Nearest Neighbors imputation approach. The resulting multifaceted array of daily physical health attributes was used to derive patient-specific recovery trajectories and infer rates of recovery surrogates (Figure 1D).

### Single-cell immune profiling

To comprehensively characterize a patient's preoperative immune state, plasma and whole blood samples were collected 1 hour before surgery for analyses with a highly multiplexed proteomic platform and single-cell mass cytometry (Figures 1B and 1C). Proteomics and immunome data from 35 patients passed quality control standards. These two platforms were

used in combination with objective physical recovery surrogates to elucidate baseline proteomic and immunological features associated with the rate of physical recovery (Figures 1E-G).

Blood for proteomic analysis was collected in EDTA tubes, placed on ice, double-spun within 60 minutes and stored at -80°C until further analysis. The proteomic analysis was performed by Olink Proteomics Inc. (Watertown, MA) with a highly multiplex platform using proximity extension technology [28]. For this study, 11 panels were used, each measuring 92 different proteins simultaneously in 1 μL of plasma. Each protein was detected by a matched pair of antibodies that were coupled to unique and partially complementary oligonucleotides. When in close proximity, a new and protein-specific DNA reporter sequence was formed by hybridization and extension, which was then amplified and quantified by real-time PCR [29]. Quality metrics were as follows: 538 of 539 plasma samples passed, 865 of 1,012 proteins were detected, and the median intra-assay coefficient of variation was 8% [30].

Blood collected for mass cytometry analysis was processed within 30 minutes after blood draw. Individual aliquots were stimulated with 5 receptor-specific ligands [i.e., granulocyte-macrophage colony-stimulating factor (GMCSF), interferon (IFN)-α, lipopolysaccharide (LPS), a mixture of interleukins (IL)-2, IL-4, and IL-6 and phorbol 12-myristate 13-acetate and ionomycin (PI)]. A 46-parameter mass cytometry assay (Supplementary Table 2, http://links.lww.com/SLA/D476) was used to analyze the distribution and intracellular signaling activities of 28 major innate and adaptive immune cell subsets (Figures 1B and 1E, Supplementary Figure 2, http://links.lww.com/SLA/D476). Intracellular mass cytometry parameters were chosen to capture important cell signaling pathways known to be activated in innate or adaptive immune cells after surgery (including JAK/STAT, P38MAPK and NFκB signaling pathways) [18], [31]. Refer to "Study Materials" in Supplementary Content for more details on mass cytometry analysis.

## Results

### An accelerometry-based clock of postoperative recovery

Tridimensional acceleration data were collected continuously in 49 patients wearing a clinical-grade ActiGraph smartwatch (ActiGraph GT9X Link, LLC, FL, USA) starting five days before and ending 40 days after surgery. The average $l2$ normalized vector magnitude of the three-dimensional data is depicted over time in Figure 1A. Each spike represents a 24-hour cycle with peak and trough activities. Magnifications of a 24-hour cycle at different postoperative days is shown in Figure 2A. Physical activity generally began increasing at 6 am and started decreasing at 6 pm reaching trough levels close to midnight. Peak and plateau activity levels continuously increased over the course of the 40-day postoperative observation period. Although there were considerable inter-personal variations in the human physical patterns after surgery, an evident steep decline followed by a gradual return in overall activity

is the dominant pattern (Figures 2A and 2C). Exceptions included light and sedentary activity, which were increased, as well as substantial disruption is the onset of sleep.

Several functional aspects were captured by the wearable sensors including a range of physical activity parameters (e.g. intensity, periods of activity, daily activity capacity, estimates of step count, estimates of caloric intake) and sleep patterns (e.g., sleep fragmentation index, sleep onset, number of awakenings). Developing time-series signal processing algorithms that extract acceleration-based functional parameters is a high-yield current research emphasis. Various algorithms were applied to extract 62 temporal physical and sleep features from the current dataset. Using a static sliding window of 24 hours, daily feature vectors were derived for each patient. The sliding window approach is a common high level feature extraction method in time series physical activity monitoring [32], [33]. To facilitate the optimization algorithm and reduce the adverse effects of outliers, a zero mean unit variance standard scaler was built on each of the preoperative data feature vectors. The scalers were then applied to the entire corresponding feature vector, independent of the other feature vectors. A correlation graph displays the complex inter-connectivity of the 62 features (Figure 2B). Each node represents one feature and edges indicate a significant pairwise statistical correlation ($p<0.01$) between nodes.

An unsupervised k-means clustering algorithm was used to objectively identify distinct components of highly correlated features. Six distinct components or domains were identified and labeled based on the included features: overall sleep, sleep onset, sleep disruption and sedentary activity, light activity, moderate and overall activity, and activity capacity (Figure 2B). The time course of the average magnitude of the six domains is shown in Figure 2C. Each domain followed a unique temporal pattern. Importantly, the domains "moderate and overall activity" and "activity capacity" sharply declined immediately after surgery and then gradually returned to preoperative levels over the course of weeks. In contrast, the domains "sleep disruption and sedentary activity" increased moderately after surgery and gradually returned to preoperative levels. This is consistent with observed decrease in "moderate and overall activity" and "activity capacity". While the domains "light activity" and "sleep onset" decreased after surgery, no clear temporal patterns were observed. Finally, the domain "overall sleep" did not noticeably change after surgery.

**Inferring patient-specific trajectories of recovery**

To quantify physical recovery patterns after surgery, the temporal postoperative accelerometry data were used to build a patient-specific model, predicting the number of 'days since surgery'. A supervised model was trained on the feature matrix of each individual patient, independently. The feature matrix consisted of 62 feature vectors of medium to high-level patient physical attributes characterizing each postoperative day as the target variable. The Random Forest (RF) regression algorithm [34] was used because of the continuity of the output variable and the highly interrelated nature of the feature vectors. RF is a robust ensemble method that allows for relatively easy interpretation of the results, leverages the specificity and non-linearity of the tree-based approaches, and takes advantage of the

generalization and robustness of ensemble methods. For each patient, a RF model was trained to infer time since surgery using the patient-specific feature matrix (as previously visualized in Figure 2B). The repeated k-fold cross-validation showed high performance of the patient-specific RF model predicting 'days since surgery' (p<0.05) with median prediction p-values of $5.9 \times 10^{-7}$ (Figure 3A, Supplementary Figure 3, http://links.lww.com/SLA/D476). Refer to the section "Modeling and Analysis" in Supplementary Content for details regarding model training and evaluation.

The performance of RF models varied between patients with a median Root Mean Square Error (RMSE) of ~8 days when estimating the 'day since surgery' (Figure 3B). Importantly, the multivariate model (shown in pink) was compared against univariate models using a single accelerometry feature as provided by the manufacturer for training the RF predictor. Six univariate models are shown in Figure 3B for manufacturer provided features (1) total steps taken in a day (24-hour period), (2) estimated daily metabolic equivalent of task, (3) number of awakening episodes detected during a patient's sleep in one day, (4) duration of time spent performing light activities, (5) onset of bedtime for a given day, and (6) total of activity counts (measured by Freedson algorithm) detected during sleep intervals for one day. The performance comparisons of all univariate models are shown in Supplementary Figure 4, http://links.lww.com/SLA/D476. Importantly, the multivariate RF models were clearly superior to the univariate models using a single accelerometry feature. As an additional control, the preoperative baseline data (before the grey dashed line) was fed into the models to predict a post-operative day. Data were normalized to baseline to ascertain within-subject control given uncertainties regarding the accuracy of absolute accelerometry metrics. This analysis demonstrated that the model's inference on the baseline (preoperative) data points ranges more than 21 days after surgery. Interestingly, this observation independently confirms the sanity of the RF models.

Figure 3C highlights the relative contribution of the 62 accelerometry features used to derive the RF model predicting 'days since surgery'. The color intensity is indicative of relative importance of each node computed using Gini importance [35]. Features in the domains 'Activity Capacity' and 'Sleep Disruption and Sedentary Activity' ranked highest followed by the features in the domains 'Moderate and Overall Activity', 'Overall Sleep', and 'Light Activity'.

An array of recovery surrogates for each patient was devised such that it quantifies the patient's recovery trajectory with respect to each accelerometry feature. The accelerometry data collected for five days preceding surgery (i.e., the baseline accelerometry feature vectors) were inputted into the personalized RF models to estimate days after surgery. Note that the baseline inferences are made by models trained solely on postoperative data. The models use the temporal patterns learned from postoperative data to infer the time point along the postoperative timeline that most closely matches baseline patterns. The RF inference on preoperative data will reveal the day after surgery that is closest to a patient's preoperative state. Based on this, an array of 62 recovery surrogates (corresponding to 62 accelerometry features) is constructed. Each element of this array (i.e., one recovery surrogate) indicates the

earliest time that the postoperative feature value returns to the patient's baseline levels. The smaller the surrogate, the faster a patient is returning to his/her preoperative physical status (as inferred from the corresponding accelerometry feature). The detailed formulation of recovery surrogates is presented in "Modeling and Analysis" section in Supplementary Content, http://links.lww.com/SLA/D476.

**Association of accelerometry-based recovery surrogates with Self-reported Outcomes**

Self-reported outcomes were captured before surgery, on postoperative days 1-3, bi-weekly after discharge for postoperative weeks 1-4, and weekly for postoperative weeks 5-6. The surgical recovery scale (SRS) and an adapted version of the Western Ontario and McMaster Universities Osteoarthritis Index (WOMAC), two extensively validated questionnaires, were used to assess general fatigue and resulting functional impairment, as well as pain and function of the operated lower extremity [19], [36], [37]. The patient-specific area under the curve (AUC) was derived for each longitudinal self-reported outcome. Refer to "Study Materials" in Supplementary Content for a detailed description of self-reported outcome tools. As shown in Figure 4, the univariate analysis revealed a significant correlation between the surgical recovery scale (SRS) and recovery surrogates derived from the proposed clock of postoperative recovery ($P < 0.003$).

**Preoperative immune states are associated with physical recovery trajectories**

A total of 1,848 mass cytometry immune features were extracted from blood samples collected before surgery. These included endogenous intracellular activities of 28 innate and adaptive immune cell subsets and their capacity to respond to the five external ligands. The immunological dataset formed a complex network of cell type-specific frequencies and signaling activities, which highlight the interconnectivity of the immune system (Figure 5A). In parallel, the concentrations of 1,008 plasma proteins were measured. The assay quantifies proteins over a wide dynamic range as normalized protein expression values (NPX), which is unit less number derived on a $log_2$ scale that is proportional to relative plasma concentrations. Similar to the immunological parameters, proteins built a complex correlational network (Figure 5B), which is annotated by gene ontology terms as provided by Olink Proteomics Inc. (Watertown, MA). The resulting immunome datasets are original and have not been reported previously.

To determine whether patients' preoperative immune and proteomic states could predict their physical recovery surrogates, Canonical-Correlation Analysis (CCA) models were trained to reveal linear associations between the physical recovery surrogates and the correlated immune or proteomic network parameters. To improve robustness, a leave-one-out cross validation algorithm was used, so that the results are predictions derived in patients not included when training the model. Refer to "Modeling and Analysis" in Supplementary Content, http://links.lww.com/SLA/D476 for detailed discussion of CCA training and evaluation. Immune network parameters predicted physical recovery surrogates of individual

patients ($p < 0.01$), while proteomic network parameters were not predictive ($p = 0.69$) as shown in Figure 5C and 5D.

Examination of the most informative immune model features (top 10% of ranked model features considering absolute coefficient) revealed intracellular signaling responses that were reminiscent of prior studies linking patients' immune response to surgery to their recovery [19]. Notably, the phosphor-(p)-STAT3 signal in monocytic myeloid-derived suppressor cells (M-MDSCs) in response to IL-2/4/6 stimulation with IL-2/4/6 positively correlated with slower physical recovery. Notably, among the 184 most informative model features, 89.6% (165 features) were negatively correlated with the physical recovery surrogate (Supplementary Table 3, http://links.lww.com/SLA/D476). Importantly, the pSTAT1 and pSTAT3 responses to INF-α stimulation in CD4T, NK and memory B cells were negatively correlated, i.e., associated with slower physical recovery.

To gain a better understanding of the correlations between specific accelerometry and immune features, additional statistical analyses considered each accelerometry feature independently (Supplementary Figure 5, http://links.lww.com/SLA/D476). Inspection of the bipartite correlation between immunological and accelerometry networks (Supplementary Figure 5A, http://links.lww.com/SLA/D476) revealed additional interconnected immunological and physical recovery parameters that change concordantly. Significant correlations were highlighted between the accelerometry and immune features using graph edges. As shown in Supplementary Figure 5B, http://links.lww.com/SLA/D476, this analysis confirmed several significant correlations between pSTAT1 response to INF- α stimulation in NK cells and CD4T cells and the "moderate and overall activity", and "activity capacity" domains.

**Discussion**

Our results indicate that wearable technologies enable the objective, scalable, and longitudinal tracking of individual patient's physical recovery after surgery. Notably, the machine-learning centered approach anchored in multivariate vector analysis offered significantly improved accuracy compared to benchmark metrics provided by manufacturers such as step count. Importantly, individual physical recovery trajectories were linked to patient-specific immune states before surgery. These findings suggest that accelerometry can be adopted as an affordable and scalable technology to track individual patient's physical recovery over time and link it to pre-surgical biological and other attributes that drive such recovery. Such insight is valuable for risk stratification and interventional strategies facilitating patients' physical recovery.

Six distinct groups of physical activity and sleep monitoring represented domains of surgical recovery. Each domain followed a unique temporal pattern. Each domain pattern indicated a noticeable disruption at the time of surgery with the exception of "Overall Sleep" domain. Features in the domains 'Activity Capacity' and 'Sleep Disruption and Sedentary Activity' were found the most informative in prediction of time after surgery and demonstrated larger

univariate correlation with recovery surrogates followed by features in the domains 'Moderate and Overall Activity'. Importantly, the highly informative "Activity Capacity" domain is supported by previous studies of using submaximal capacity parameters such as "5-Chair Stand and Timed Up and Go" in assessment of physical performance and surgical recovery [38]. This result warrants studying similar physical performance attributes in a continuous and pervasive fashion.

The proposed recovery surrogates derived from the wearable data demonstrated a significant correlation with the self-reported SRS. The SRS is specifically designed to capture surgical recovery as it measures attributes of fatigue and resulting functional consequences on daily activities in surgical patients [36], [39]. The SRS is sensitive to change and correlates with course and severity of postoperative complications [19], [40]. Importantly, this result provides validation that the accelerometry derived surrogates resonate with a relevant patient reported outcome.

The canonical-correlation analysis revealed immune correlates of clinical recovery that echoed findings of previous studies [18], [31]. Importantly, the pSTAT3 signal activity in M-MDSCs predicted a slower recovery. M-MDSCs are a monocyte subset with suppressive capacity that expand in the context of certain malignancies, sepsis and traumatic injury [41]–[43]. Prior *in vitro* and *in vivo* studies suggest that STAT3 is an essential transcription factor for M-MDSCs to suppress the proliferation and function of CD4T cells and other immune cells, including NK cells [44]. In the context of surgery, our group previously showed that the pSTAT3 signal in M-MDSCs strongly correlated with prolonged postoperative functional recovery [19]. As such, the derived recovery surrogates can reveal biological determinants of surgical recovery.

Additional analysis in Supplementary Figure 5, http://links.lww.com/SLA/D476 revealed negative correlations between preoperative adaptive immune responses and the rate of postoperative recovery. They included the STAT1 and STAT6 signaling responses to IFN-α in B and CD4T cell subsets (particularly related to "moderate and overall activity" and "activity capacity" domains). Type I IFN-α stimulation lowers the threshold for adaptive cell activation, especially by inducing up-regulation of CD69, CD86 and CD25 receptors [45]. Interestingly, adaptive cells such as B and T cells are well described as being key elements in bone [46], [47] and wound healing [48]. They also included the STAT1 response to IFN-α stimulation in NK cells. Taken together, the results suggest that preoperative immune states characterized by increased JAK/STAT signaling in B cell, CD4+T cell and NK cell and decreased JAK/STAT signaling in M-MDSC JAK/STAT benefit patients' physical recovery trajectory. An important next step is to examine whether selective modulation of the JAK/STAT signaling pathways before surgery can accelerate physical recovery.

This study has several limitations. While the models were cross-validated and tested on previously unseen patients, the relatively small sample size limits the generalizability of our results. As such, larger studies are required to independently validate our results and test the boundaries of their generalizability. The study was conducted in patients undergoing major

joint replacement surgery. As such, larger studies are likely needed to develop models generalizable across, or specific to, various surgery types. Finally, the pre-operative period was limited to only one week. We note that data during this week prior to surgery are likely impacted by pain and impairment and do not represent baseline activity levels of cohort not suffering from osteoarthritis. However, a post-hoc analysis demonstrated that our results were not confounded by preoperative activity levels (Supplementary Figure 6, http://links.lww.com/SLA/D476).

Taken together, to the best of our knowledge this is the first study to combine wearable technologies, machine learning approaches, and state-of-the-art immune monitoring to describe patient-specific physical recovery trajectories that outperform benchmark metrics and provide insight into biology that may drive important aspects of postoperative recovery. The outlined strategy is scalable and therefore amenable for implementation in larger-scale studies providing more detailed and generalizable insight into perioperative patient factors that drive clinical recovery.

**Reproducibility and Data Availability**

Data and source codes for reproduction of the results are publicly available at https://github.com/raminfl/hipval. ActiGraph's actigraphy data analysis software platform ActiLife v6.13.3 can be downloaded from https://actigraphcorp.com/actilife

**References**

[1]     T. G. Weiser *et al.*, "Size and distribution of the global volume of surgery in 2012," *Bull. World Health Organ.*, 2016, doi: 10.2471/blt.15.159293.

[2]     H. Kehlet and J. B. Dahl, "Anaesthesia, surgery, and challenges in postoperative recovery," *Lancet*, vol. 362, no. 9399, pp. 1921–1928, Dec. 2003, doi: 10.1016/S0140-6736(03)14966-5.

[3]     M. B. Jensen, K. B. Houborg, C. B. Nørager, M. G. Henriksen, and S. Laurberg, "Postoperative changes in fatigue, physical function and body composition: An analysis of the amalgamated data from five randomized trials on patients undergoing colorectal surgery," *Color. Dis.*, 2011, doi: 10.1111/j.1463-1318.2010.02232.x.

[4]     T. Bisgaard, B. Klarskov, J. Rosenberg, and H. Kehlet, "Characteristics and prediction of early pain after laparoscopic cholecystectomy," *Pain*, 2001, doi: 10.1016/S0304-3959(00)00406-1.

[5]     M. A. Aarts, A. Okrainec, A. Glicksman, E. Pearsall, J. Charles Victor, and R. S. McLeod, "Adoption of enhanced recovery after surgery (ERAS) strategies for colorectal surgery at academic teaching hospitals and impact on total length of hospital stay," *Surg. Endosc.*, 2012, doi: 10.1007/s00464-011-1897-5.

[6]     H. Kehlet and D. W. Wilmore, "Evidence-Based Surgical Care and the Evolution of Fast-Track Surgery," *Ann. Surg.*, vol. 248, no. 2, pp. 189–198, Aug. 2008, doi: 10.1097/SLA.0b013e31817f2c1a.

[7]     L. Lee, T. Tran, N. E. Mayo, F. Carli, and L. S. Feldman, "What does it really mean to 'recover' from an operation?," *Surgery*, vol. 155, no. 2, pp. 211–216, Feb. 2014, doi: 10.1016/j.surg.2013.10.002.

[8]     G. Bishwajit, D. P. O'Leary, S. Ghosh, S. Yaya, T. Shangfeng, and Z. Feng, "Physical inactivity and self-reported depression among middle- and older-aged population in South Asia: World health survey," *BMC Geriatr.*, 2017, doi: 10.1186/s12877-017-0489-1.

[9]     A. Bauman *et al.*, "The descriptive epidemiology of sitting: A 20-country comparison using the international physical activity questionnaire (IPAQ)," *Am. J. Prev. Med.*, 2011, doi: 10.1016/j.amepre.2011.05.003.

[10]    Y. Tarasenko, C. Chen, and N. Schoenberg, "Self-Reported Physical Activity Levels of Older Cancer Survivors: Results from the 2014 National Health Interview Survey," *J. Am. Geriatr. Soc.*, 2017, doi: 10.1111/jgs.14589.

[11]    C. J. Killen, M. P. Murphy, W. J. Hopkinson, M. A. Harrington, W. H. Adams, and H. W. Rees, "Minimum twelve-year follow-up of fixed- vs mobile-bearing total knee arthroplasty: Double blinded randomized trial," *J. Clin. Orthop. Trauma*, 2020, doi: 10.1016/j.jcot.2019.03.019.

[12]    S. A. Prince, K. B. Adamo, M. E. Hamel, J. Hardt, S. Connor Gorber, and M. Tremblay, "A comparison of direct versus self-report measures for assessing physical activity in adults: A systematic review," *International Journal of Behavioral Nutrition and Physical Activity*. 2008, doi: 10.1186/1479-5868-5-56.

[13]    E. Cerin *et al.*, "Correlates of agreement between accelerometry and self-reported physical activity," *Med. Sci. Sports Exerc.*, 2016, doi: 10.1249/MSS.0000000000000870.

[14]    P. C. Hallal, L. B. Andersen, F. C. Bull, R. Guthold, W. Haskell, and U. Ekelund, "Global physical activity levels: surveillance progress, pitfalls, and prospects," *Lancet*, vol. 380, no. 9838, pp. 247–257, Jul. 2012, doi: 10.1016/S0140-6736(12)60646-1.

[15]    M. Cornacchia, K. Ozcan, Y. Zheng, and S. Velipasalar, "A Survey on Activity Detection and Classification Using Wearable Sensors," *IEEE Sens. J.*, 2017, doi: 10.1109/JSEN.2016.2628346.

[16]    J. Conci, G. Sprint, D. Cook, and D. Weeks, "Utilizing Consumer-grade Wearable Sensors for Unobtrusive Rehabilitation Outcome Prediction," in *2019 IEEE EMBS*

*International Conference on Biomedical & Health Informatics (BHI)*, May 2019, pp. 1–4, doi: 10.1109/BHI.2019.8834512.

[17]   W. Xiao *et al.*, "A genomic storm in critically injured humans," *J. Exp. Med.*, 2011, doi: 10.1084/jem.20111354.

[18]   B. Gaudilliere *et al.*, "Coordinated Surgical Immune Signatures Contain Correlates of Clinical Recovery," *Sci Transl Med*, 2014, doi: 10.1126/scitranslmed.3009701.

[19]   B. Gaudilliere *et al.*, "Clinical recovery from surgery correlates with single-cell immune signatures," *Sci. Transl. Med.*, vol. 6, no. 255, pp. 255ra131-255ra131, Sep. 2014, doi: 10.1126/scitranslmed.3009701.

[20]   S. C. Bendall, G. P. Nolan, M. Roederer, and P. K. Chattopadhyay, "A deep profiler's guide to cytometry," *Trends in Immunology*. 2012, doi: 10.1016/j.it.2012.02.010.

[21]   E. W. Newell, N. Sigal, N. Nair, B. A. Kidd, H. B. Greenberg, and M. M. Davis, "Combinatorial tetramer staining and mass cytometry analysis facilitate T-cell epitope mapping and characterization," *Nat. Biotechnol.*, 2013, doi: 10.1038/nbt.2593.

[22]   A. Olin *et al.*, "Stereotypic Immune System Development in Newborn Children," *Cell*, 2018, doi: 10.1016/j.cell.2018.06.045.

[23]   N. Aghaeepour *et al.*, "An immune clock of human pregnancy," *Sci. Immunol.*, vol. 2, no. 15, p. eaan2946, Sep. 2017, doi: 10.1126/sciimmunol.aan2946.

[24]   M. H. Spitzer *et al.*, "Systemic Immunity Is Required for Effective Cancer Immunotherapy," *Cell*, 2017, doi: 10.1016/j.cell.2016.12.022.

[25]   G. K. Fragiadakis *et al.*, "Patient-specific Immune States before Surgery Are Strong Correlates of Surgical Recovery.," *Anesthesiology*, vol. 123, no. 6, pp. 1241–55, Dec. 2015, doi: 10.1097/ALN.0000000000000887.

[26]   R. J. Cole, D. F. Kripke, W. Gruen, D. J. Mullaney, and J. C. Gillin, "Automatic Sleep/Wake Identification From Wrist Activity," *Sleep*, vol. 15, no. 5, pp. 461–469, Sep. 1992, doi: 10.1093/sleep/15.5.461.

[27]   P. S. Freedson, E. Melanson, and J. Sirard, "Calibration of the Computer Science and Applications, Inc. accelerometer," *Med. Sci. Sports Exerc.*, 1998, doi: 10.1097/00005768-199805000-00021.

[28]   E. Assarsson *et al.*, "Homogenous 96-Plex PEA Immunoassay Exhibiting High Sensitivity, Specificity, and Excellent Scalability," *PLoS One*, vol. 9, no. 4, p. e95192, Apr. 2014, doi: 10.1371/journal.pone.0095192.

[29] Olink Proteomics Inc., "PEA – a high-multiplex immunoassay technology with qPCR or NGS readout," *White Pap. v1.0*, 2020.

[30] Olink Proteomics Inc., "Data normalization and standardization," *White Pap. v1.0*, 2018.

[31] E. A. Ganio *et al.*, "Preferential inhibition of adaptive immune system dynamics by glucocorticoids in patients after acute surgical trauma," *Nat. Commun.*, vol. 11, no. 1, pp. 1–12, Dec. 2020, doi: 10.1038/s41467-020-17565-y.

[32] N. C. Krishnan and D. J. Cook, "Activity recognition on streaming sensor data," *Pervasive Mob. Comput.*, 2014, doi: 10.1016/j.pmcj.2012.07.003.

[33] S. J. Preece, J. Y. Goulermas, L. P. J. Kenney, and D. Howard, "A comparison of feature extraction methods for the classification of dynamic activities from accelerometer data," *IEEE Trans. Biomed. Eng.*, 2009, doi: 10.1109/TBME.2008.2006190.

[34] P. Geurts, D. Ernst, and L. Wehenkel, "Extremely randomized trees," *Mach. Learn.*, 2006, doi: 10.1007/s10994-006-6226-1.

[35] L. Breiman, "Random forests," *Mach. Learn.*, 2001, doi: 10.1023/A:1010933404324.

[36] J. S. Paddison, T. Sammour, A. Kahokehr, K. Zargar-Shoshtari, and A. G. Hill, "Development and validation of the surgical recovery scale (SRS)," *J. Surg. Res.*, 2011, doi: 10.1016/j.jss.2010.12.043.

[37] N. Bellamy, W. W. Buchanan, C. H. Goldsmith, J. Campbell, and L. W. Stitt, "Validation study of WOMAC: a health status instrument for measuring clinically important patient relevant outcomes to antirheumatic drug therapy in patients with osteoarthritis of the hip or knee.," *J. Rheumatol.*, vol. 15, no. 12, pp. 1833–40, Dec. 1988.

[38] H. Master *et al.*, "Physical Performance Tests Provide Distinct Information in Both Predicting and Assessing Patient-Reported Outcomes Following Lumbar Spine Surgery," *Spine (Phila. Pa. 1976).*, vol. 45, no. 23, pp. E1556–E1563, Dec. 2020, doi: 10.1097/BRS.0000000000003665.

[39] J. S. Paddison, R. J. Booth, A. G. Hill, and L. D. Cameron, "Comprehensive assessment of peri-operative fatigue: development of the Identity-Consequence Fatigue Scale," *J. Psychosom. Res.*, vol. 60, no. 6, pp. 615–622, Jun. 2006, doi: 10.1016/j.jpsychores.2005.08.008.

[40] P. P. Singh, S. Srinivasa, D. P. Lemanu, A. A. Kahokehr, and A. G. Hill, "The Surgical Recovery Score correlates with the development of complications following elective

colectomy," *J. Surg. Res.*, 2013, doi: 10.1016/j.jss.2012.12.005.

[41]  A. G. Cuenca *et al.*, "A paradoxical role for myeloid-derived suppressor cells in sepsis and trauma," *Mol. Med.*, vol. 17, no. 3–4, pp. 281–292, Mar. 2011, doi: 10.2119/molmed.2010.00178.

[42]  N. Aghaeepour *et al.*, "Deep Immune Profiling of an Arginine-Enriched Nutritional Intervention in Patients Undergoing Surgery," *J. Immunol.*, vol. 199, no. 6, pp. 2171–2180, Sep. 2017, doi: 10.4049/jimmunol.1700421.

[43]  S. Nagaraj *et al.*, "Regulatory myeloid suppressor cells in health and disease," in *Cancer Research*, Oct. 2009, vol. 69, no. 19, pp. 7503–7506, doi: 10.1158/0008-5472.CAN-09-2152.

[44]  A. Stiff *et al.*, "Nitric oxide production by myeloid-derived suppressor cells plays a role in impairing Fc receptor–mediated natural killer cell function," *Clin. Cancer Res.*, vol. 24, no. 8, pp. 1891–1904, Apr. 2018, doi: 10.1158/1078-0432.CCR-17-0691.

[45]  D. Braun, I. Caramalho, and J. Demengeot, "IFN-α/β enhances BCR-dependent B cell responses," *Int. Immunol.*, vol. 14, no. 4, pp. 411–419, Apr. 2002, doi: 10.1093/intimm/14.4.411.

[46]  H. Takayanagi, "Osteoimmunology: Shared mechanisms and crosstalk between the immune and bone systems," *Nature Reviews Immunology*, vol. 7, no. 4. Nature Publishing Group, pp. 292–304, Apr. 2007, doi: 10.1038/nri2062.

[47]  I. Könnecke *et al.*, "T and B cells participate in bone repair by infiltrating the fracture callus in a two-wave fashion," *Bone*, vol. 64, pp. 155–165, Jul. 2014, doi: 10.1016/j.bone.2014.03.052.

[48]  Y. Iwata *et al.*, "CD19, a response regulator of B lymphocytes, regulates wound healing through hyaluronan-induced TLR4 signaling," *Am. J. Pathol.*, vol. 175, no. 2, pp. 649–660, 2009, doi: 10.2353/ajpath.2009.080355.

**Figure 1. Study overview and analytical approach.** Forty-nine patients undergoing hip replacement surgery were included in the analysis. **(A)** Patients were instructed to wear a clinical grade motion sensing smart-watch continuously on their wrist for 5 days before and for 40 days after surgery to monitor physical activity and sleep patterns. **(B)** Whole blood samples were obtained from each patient one hour before surgery for analysis with mass cytometry to determine immune cell-type specific signaling activities at baseline and in response to ex-vivo stimulation with the receptor-specific ligands granulocyte-macrophage colony-stimulating factor (GMCSF), interferon alpha (INF- α), interleukins 2, 4 and 6 (IL), lipopolysaccharide (LPS), and a mixture of phorbol 12-myristate 13-acetate and ionomycin (PI) **(C)** An antibody-based proteomic platform was used for measuring 1,012 proteins in plasma of the same samples. **(D)** Patient-specific daily activity and sleep patterns adjusted to preoperative metrics were used for inferring model parameters reflecting the rate of recovery, i.e., the time to return to preoperative states. Correlation networks were built for **(E)** mass cytometry and **(F)** proteomic data sets. **(G)** The feature sets presented in the correlation networks trained multivariate models predicting the rate of recovery based on patients' preoperative immune and proteomic states.
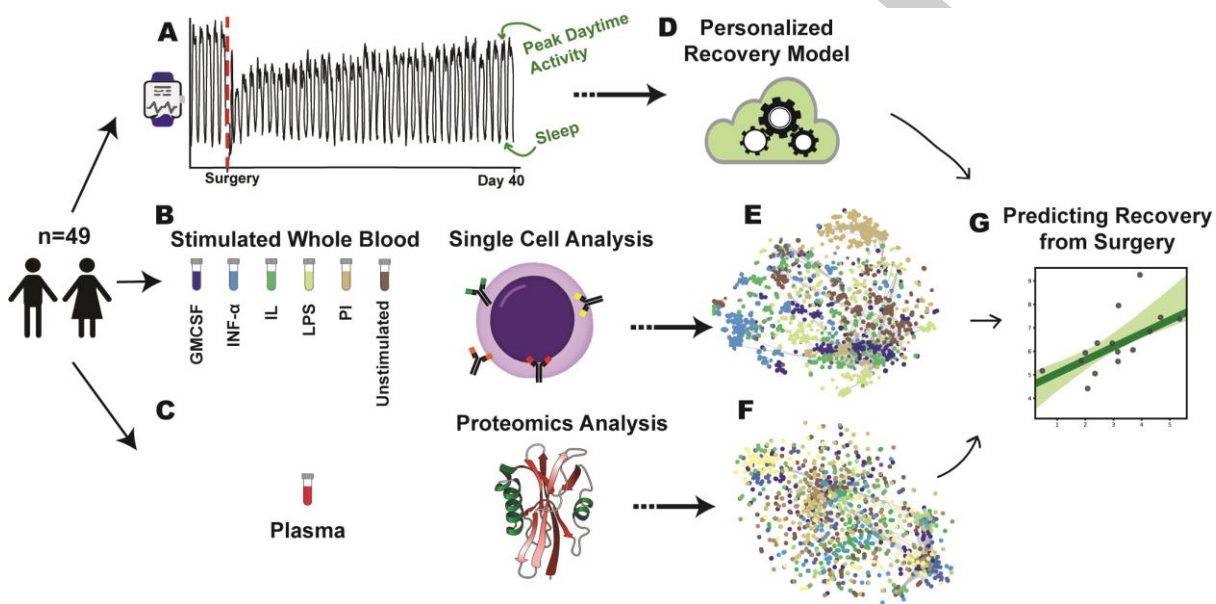
**Figure 2. Accelerometer signal processing and feature extraction.** (**A**) Depicted is the average normalized (l2 norm) vector magnitude of high-fidelity three-dimensional acceleration measurements recorded over distinct 24-hour periods. Color-coded lines track the signal magnitude at different postoperative days. (**B**) The correlation network of relevant activity and sleep parameters (nodes) reveals distinct components derived by applying an unsupervised clustering algorithm (kMeans). Major components of the network included moderate and overall activity (orange), activity capacity (blue), light activity (yellow), overall sleep attributes (ocean green), sleep onset (lawn green), and sleep disruption overlapping with sedentary activity (pink). Node sizes indicate the strength of the correlation between a parameter and the number of days after surgery. The edges indicate statistical significance ($p < 0.01$, Spearman's correlation). (**C**) Shown is the average magnitude for each component over the course of the observation period starting 5 days before and ending 40 days after surgery. The color code is identical with (B), shaded areas mark the 90% confidence intervals, the horizontal grey line indicates the average before surgery, and the vertical grey line indicates the day of surgery.
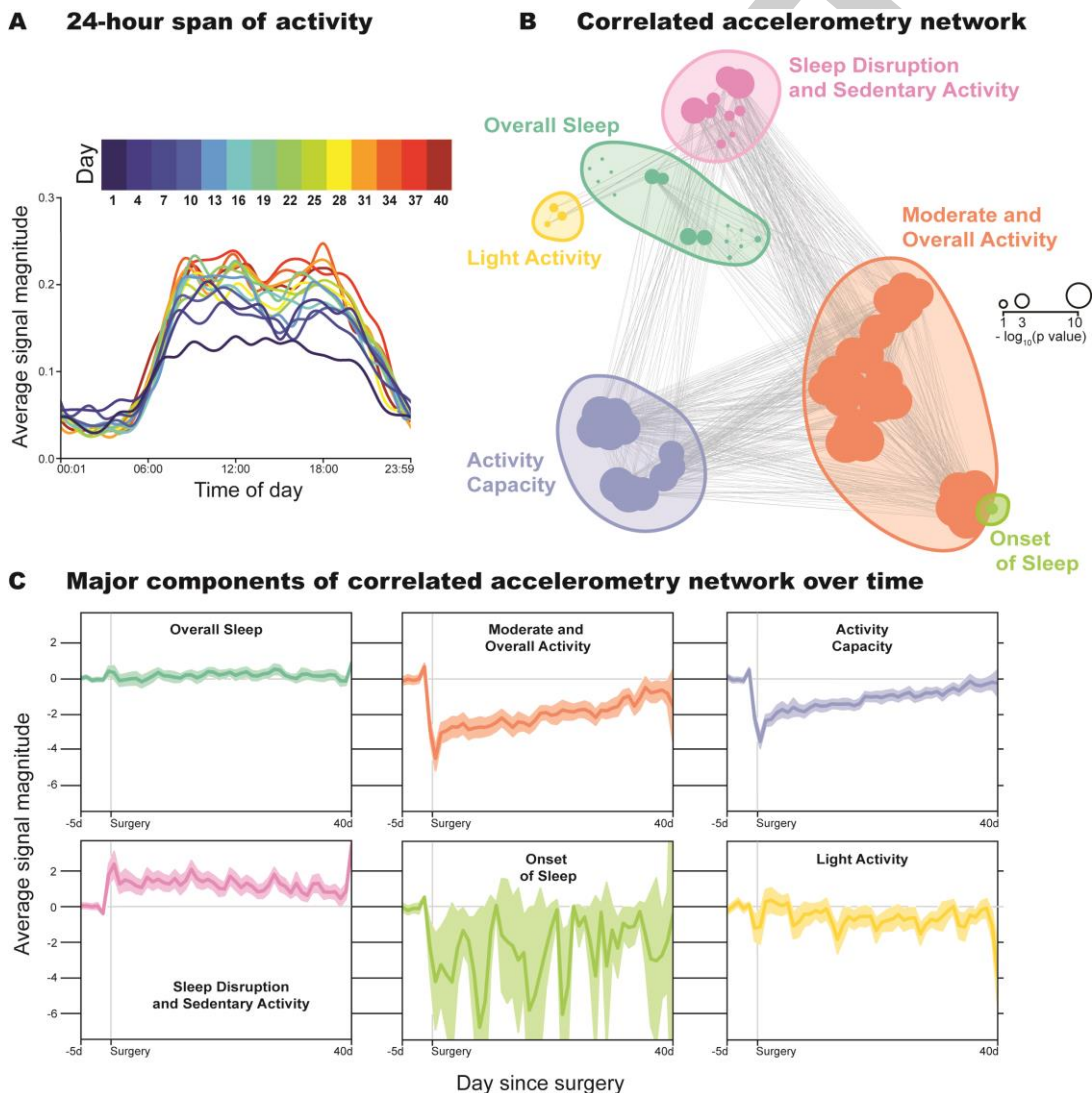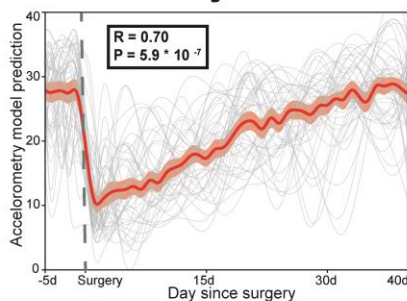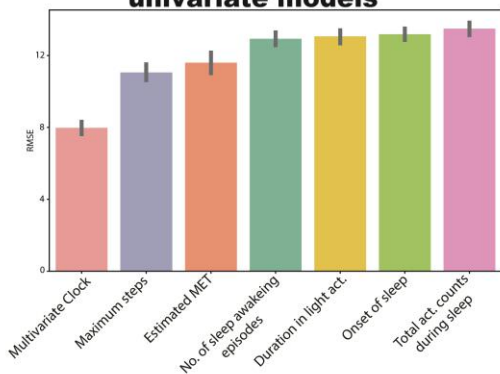
**Figure 3. An accelerometry clock of recovery from surgery.** **(A)** The patient-specific correlated accelerometry network of temporal physical activity and sleep quality features was used to predict 'days since surgery' (Spearman's $\rho = 0.7, p = 5.9 \times 10^{-7}$, cross validation). The model predictions versus ground truth 'Day since surgery' is plotted. Personalized model predictions are shown in grey (n=49). The mean predictions and 90% confidence intervals are shown in red. The vertical dashed line indicates the day of surgery. **(B)** The multivariate clock of recovery in (A) is compared against univariate models using metrics provided by the manufacturer. The y axis depicts the median Root Mean Square Error and the black line atop each bar depicts the 90% CI. **(C)** The correlated accelerometry network shows the major domains of accelerometry-derived attributes (daily sleep and activity). The color of the nodes corresponds to the relative contribution of each component to the cross-validated model predicting 'days since surgery' (i.e., gini importance). The darker shades indicate higher importance.
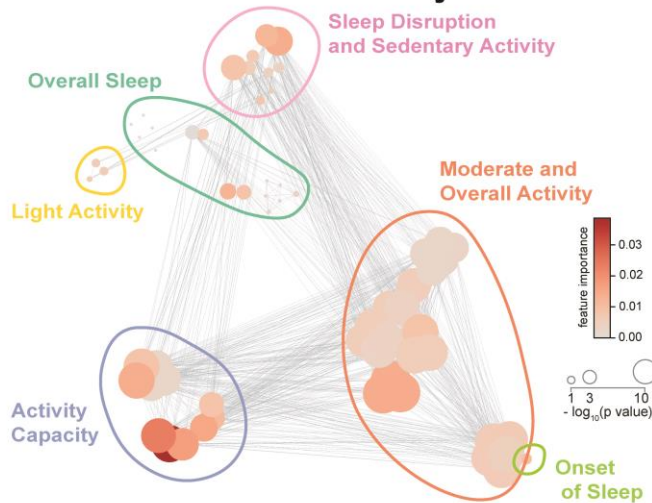
**Figure 4. Correlation with self-reported clinical outcomes.** The univariate correlation (spearman's) between patients' objective physical recovery trajectory, and questionnaire-based subjective outcomes including fatigue (SRS), pain and function of the operated limb (WOMAC), and comorbidity burden (index) are shown. Fatigue and physical recovery trajectories correlated significantly ($p < 0.003$).
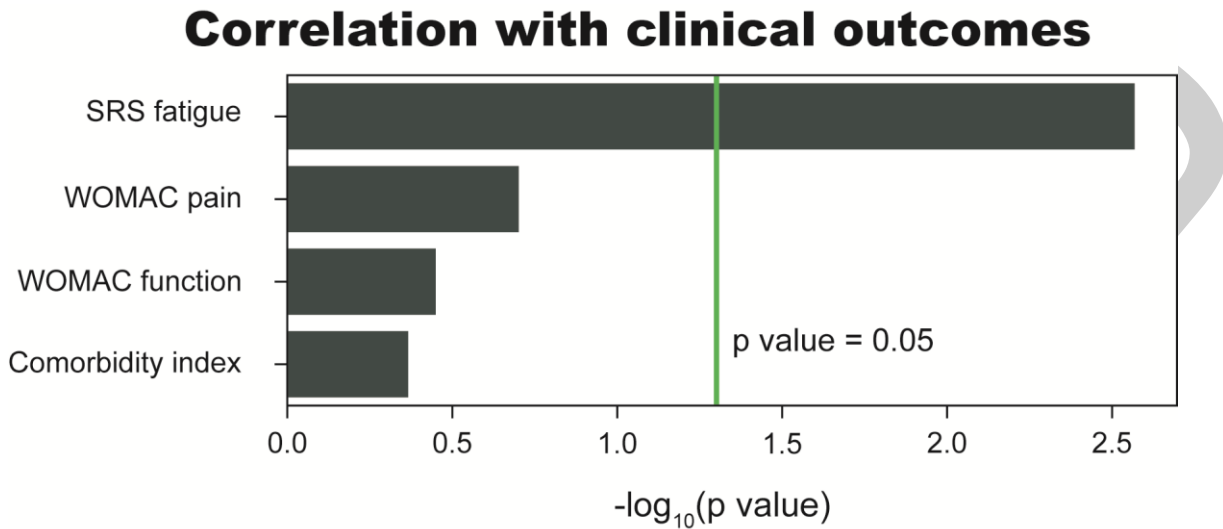
**Figure 5. Preoperative immune parameters predict patient-specific physical recovery trajectories. (A)** The immune correlation network within and across various features is color-coded to reflect cellular phenotypical and functional basal conditions as well as cellular responses to ex-vivo stimulation with different ligands including granulocyte-macrophage colony-stimulating factor (GMCSF), interferon alpha (INF- α), interleukins (IL) -2, -4 and -6, lipopolysaccharide (LPS), and a mixture of phorbol 12-myristate 13-acetate (PMA), ionomycin (PI). **(B)** The proteomic correlation network is colored by gene ontology terms. **(C)** Preoperative immune network parameters predict physical recovery trajectories ($R = 0.46, p = 5.2 \times 10^{-3}$). The shaded area denotes the 90% confidence interval of the regression line (solid black). **(D)** Preoperative proteomic network parameters were not predictive.
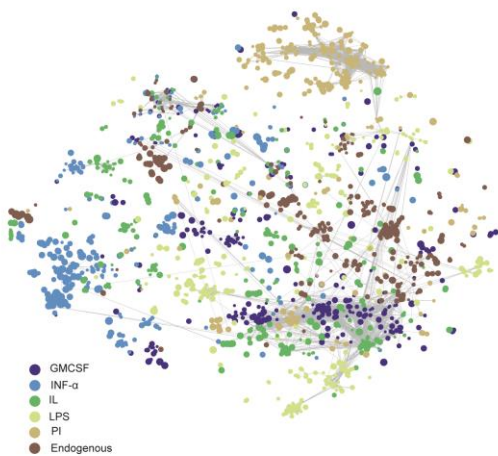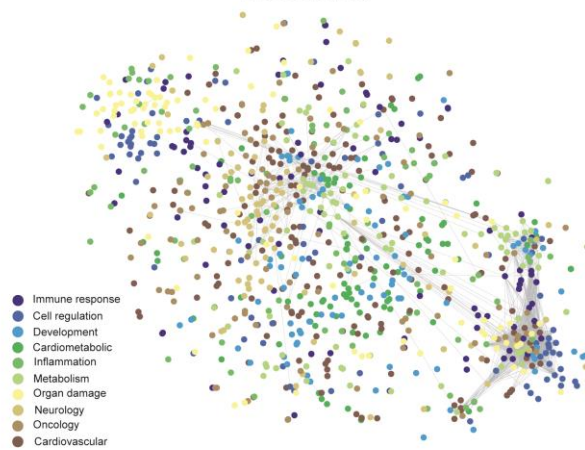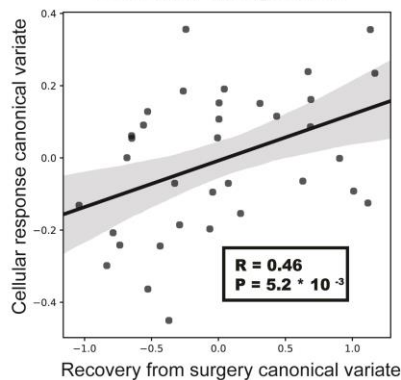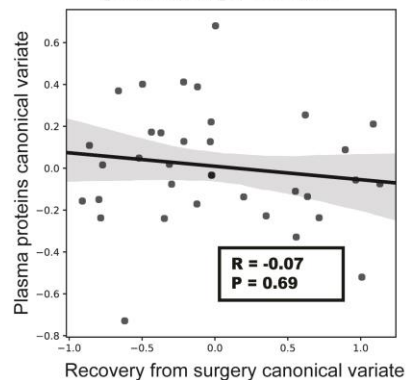
**Table 1: Patient Data**

| DEMOGRAPHICS AND PRESURGICAL CLINICAL CHARACHTERISTICS | |
|---|---|
| Sex (male/female) | 23/26 |
| Age (years; median & IQR) | 63 (57-68) |
| Body mass index (kg/m$^2$; median & IQR) | 26.7 (24.2-30.5) |
| Race | |
|     African American | 1 |
|     Asian | 2 |
|     Caucasian | 42 |
|     Unknown | 4 |
| Cumulative Illness Rating Scale (0-56; median & IQR) | 10 (7-12) |
| Beck Depression Inventory (0-63; median & IQR) | 7 (5-14) |
| Profile of Moods Anxiety Scale (0-36; median & IQR | 7 (3-11) |
| 10-Itme Stress Scale (0-40; median & IQR) | 12 (6-18) |
| 36-Item Short Form Health Survey (median & IQR) | |
|     Physical component summary score (15.0-61.7) | 33.9 (30.0-38.0) |
|     Mental component summary score (7.4-65.6) | 42.7 (35.9-52.8) |
| | |
| Surgical Recovery Scale (17-100; median & IQR) | 63.7 (54.1-72.6) |
| Western Ontario and McMaster Universities Osteoarthritis Index (median & IQR) | |
|     Hip pain (0-40) | 21.5 (15.5-28.5) |
|     Hip function (0-60) | 32.5 (23.0-42.0) |
| Hip Disability and Osteoarthritis Outcomes Score (0-100; median & IQR) | |
|     Pain | 45.0 (32.5-52.5) |
|     Symptom | 35.0 (20.0-50.0) |
|     Activity of daily living | 50.0 (32.0-60.0) |
|     Sport | 18.8 (6.3-31.3) |
|     Quality of life | 19.0 (6.0-31.0) |
| ANESTHESIA AND SURGERY | |

|  |  |
|---|---|
| ASA class (1-5; median & IQR) | 2 (2-3) |
| Anesthetic technique | |
| General & Neuraxial | 30 |
| General | 10 |
| Neuraxial | 9 |
| Times (min; median & IQR) | |
| Surgery | 102 (81-113) |
| Anesthesia | 183 (158-198) |
| Post anesthesia care unit | 103 (82-148) |
| Blood loss (ml; median & IQR) | 300 (200-300) |
| Intraoperative fluids (ml; median & IQR) | 1500 (1000-2000) |
| Opioid use postoperative day 1&2 (mg; median & IQR) [1] | 7.5 (3.4-12.0) |
| Time to discharge (days; median & IQR) | 2.1 (2.0-2.9) |

1) Intravenous hydromorphone equivalent